Vol. 137 (2020) ACTA PHYSICA POLONICA A No. 4

Special issue: ICCESEN-2019

Physical Properties of the Binary Mixtures of Ethanol + Benzene and Ethanol + Pyridine at Five Temperatures under Atmospheric Pressure

F. Aliaj[a], A. Gjevori[b], N. Syla[a], N. Elezaj[a], B. Ziberi[c] and B. Dalipi[d,*]
[a]University of Prishtina, Department of Physics, Eqrem Çabej Str. 51, 10000 Prishtina, Kosovo
[b]Polytechnic University of Tirana, Department of Physical Engineering,
Mother Theresa Square No. 4, 1000 Tirana, Albania
[c]State University of Tetovo, Faculty of Natural Sciences and Mathematics, Department of Physics,
Ilinden Str., 1200 Tetovo, North Macedonia
[d] University "Kadri Zeka", Faculty of Education, Zija Shemsiu Str. 03, 60000 Gjilan, Kosovo

Experimental densities and speeds of sound at temperatures 293.15, 298.15, 303.15, 308.15, and 318.15 K and viscosities at 298.15 K are reported in this paper for the binary liquid mixtures of ethanol + benzene and ethanol + pyridine over the entire composition range and atmospheric pressure. From these experimental data, the excess molar volumes, V^E, deviations in viscosity, $\Delta\eta$, and isentropic compressibility $\Delta\kappa_s$ were calculated and fitted by the Redlich–Kister polynomial to determine the adjustable fitting parameters and the standard deviations. The optimal number of adjustable parameters to be included in a Redlich–Kister polynomial for fitting thermodynamic excess and deviation data has been determined through F-test. The variation of excess and deviation functions with composition and temperature has been interpreted in terms of molecular interactions between the components of the mixture and structural effects.

DOI: 10.12693/APhysPolA.137.465

PACS/topics: physical properties, Redlich–Kister polynomial, binary mixture, F-test

1. Introduction

Knowledge of physical properties (such as density, speed of sound, and viscosity) of liquid mixtures is essential for the understanding of molecular interactions existing between various species in a mixture, and thus the experimental determination of physical properties at different temperatures covering the whole composition range is almost a necessity from both theoretical and practical point of view [1–7].

The particular substances were chosen due to their importance in various chemical and industrial processes. Benzene C_6H_6 is a non-polar aromatic hydrocarbon, and serves as an intermediate to the production of many substances that find uses in the manufacture of plastics, for the chemistry of dyestuffs, as well as for the manufacture of pharmaceuticals [8].

Pyridine C_6H_5N is structurally analogous to benzene, with one methine group (=CH—) being replaced by an N atom. However, in contrast to benzene, pyridine exhibits a permanent dipole moment that is traceable to the higher electronegativity of N compared with C [9]. Pyridine is used as a solvent in the manufacture of rubber and dyes, and as an intermediate for the synthesis of many drugs, insecticides, and herbicides [10, 11].

Ethanol C_2H_5OH is an excellent solvent and essential industrial ingredient. It is widely used as a precursor to the production of other organic compounds, as well as a potential clean fuel to substitute for petroleum fuels due to its low level of soot emission [12]. Ethanol is a polar liquid, strongly self-associated by hydrogen-bonded linear chains (OH• • •HO interactions) to the extent of polymerization that may differ depending on the temperature [3, 5]. Mixing ethanol with aromatic hydrocarbons would induce dissociation of some of the hydrogen-bonded structures leading to the possibility of formation of weak π•••HO bonding between the π-electron cloud of the aromatic ring and the proton of the hydroxyl group of ethanol. Weak hydrogen bonding of aromatic rings with proton donors (like ethanol) plays an essential role in the structure of certain biomolecules [13].

The aforementioned considerations led us to undertake the present work, which is in continuation of our systematic research program concerning various physical properties of binary and ternary liquid mixtures containing important compounds [14–18]. Here we report experimental densities and speed of sounds of binary liquid mixtures of ethanol with benzene or pyridine over the entire composition range at five temperatures 293.15, 298.15, 303.15, 308.15, and 313.15 K under local atmospheric pressure. The dynamic viscosities of these mixtures have also been measured at 298.15 K. Experimental data were then used to derive excess molar volumes, deviations in isentropic compressibility, and viscosity deviations from ideal behaviour over the entire composition range.

---

*corresponding author; e-mail:
bashkim.dalipi@uni-gjilan.net

2. Materials and methods

Ethanol (≥99.9%), benzene (≥99.7%), and pyridine (≥99.5%) were all obtained from Sigma-Aldrich® and were used as supplied. The purity of these chemicals was ascertained by measuring their physical properties (density, speed of sound, and viscosity) and comparing them with literature values. These data are in good agreement with literature values, as given in Table I at 298.15 K only.

Fourteen mixtures of ethanol + benzene and eighteen mixtures of ethanol + pyridine have been prepared to cover the whole mole fraction range. The mole fraction uncertainty of the studied mixtures was estimated to be within ±0.0001. All mixtures were prepared just before use for measurements of density, speed of sound and viscosity. Density and speed of sound were studied at T = 293.15, 298.15, 303.15, 308.15, and 313.15 K, and viscosity at 298.15 K only, under local atmospheric pressure of ≈ 95 kPa.

The densities ρ and speeds of sound u of pure liquids and their binary mixtures were measured by using a DSA 5000M digital vibrating U-tube densimeter (Anton Paar, Graz, Austria), automatically thermostatted within ±0.001 K. The precision/accuracy of this instrument is $\pm 0.001/\pm 0.007$ kg m^{-3} for density, and $\pm 0.01/\pm 0.1$ m s^{-1} for speed of sound measurements. Calibration of the instrument was performed periodically with dry air and Anton Paar's ultrapure water. The dynamic viscosities η were measured using a calibrated Cannon-Fenske viscometer with two measuring bulbs. Prior to making the flow-time measurements, the viscometer with the test liquid was allowed to stand for 30 min in a water bath the temperature of which was maintained at 298.15 ±0.04 K. Measurements were repeated ten times, five for each bulb, and averages were considered in all calculations. Uncertainties in the measured viscosities were within ±0.002 mPa s.

3. Results and discussions

The experimental values of density ρ, speed of sound u, dynamic viscosity η, and calculated excess molar volumes V^E, deviations in isentropic compressibility $\Delta\kappa_S$, and viscosity deviations $\Delta\eta$, at different temperatures and atmospheric pressure for ethanol + benzene and ethanol + pyridine mixtures, are listed in Tables II–IV against the mole fraction of ethanol x_1.

The excess molar volumes were calculated from density data by the following relation [3, 5, 6, 15]:

$$V^E = \sum_{i=1}^{2} x_i M_i \left(\rho^{-1} - \rho_i^{-1}\right), \tag{1}$$

where ρ is the density of the mixture, and x_i, M_i, and ρ_i are the mole fraction, molar mass, and density of the pure component i, respectively.

The viscosity deviations have been calculated by [3–7]:

$$\Delta\eta = \eta - \sum_{i=1}^{2} x_i \eta_i, \tag{2}$$

where η and η_i are the dynamic viscosity of the mixture and of pure component i, respectively.

The deviations in isentropic compressibility were calculated from experimental values of density and speed of sound data by using the following equations [3, 5]:

$$\kappa_S = \left(\rho u^2\right)^{-1}, \tag{3}$$

$$\varphi_i = \frac{x_i M_i \rho_i^{-1}}{\sum_j x_j M_j \rho_j^{-1}}, \tag{4}$$

$$\Delta\kappa_S = \kappa_S - \sum_{i=1}^{2} \varphi_i \kappa_{S,i}, \tag{5}$$

where φ_i, κ_S, and $\kappa_{S,i}$ are the volume fraction, isentropic compressibility of the mixture and of the pure component i, respectively.

The dependence of $\Delta\kappa_S$ on the volume fraction of ethanol, φ_1, and that of V^E and $\Delta\eta$ on the mole fraction of ethanol, x_1, are plotted in Figs. 1–3. The $\Delta\kappa_S$ and V^E values are negative over the entire composition range for the ethanol + pyridine system, whereas for the mixtures of ethanol with benzene the $\Delta\kappa_S$ and V^E vary much like a sigmoidal S-shaped curve with positive values at lower ethanol concentrations and negative values at higher ethanol concentrations. The minima of the $\Delta\kappa_S$–φ_1 and V^E–x_1 curves for the ethanol + pyridine mixtures occur at $\varphi_1 \approx 0.57$ and $x_1 \approx 0.6$, respectively.

TABLE I

Physical properties (density ρ, speed of sound u, and viscosity η) of the pure liquids as measured in our laboratory and those reported in the literature at 298.15 K and atmospheric pressure.

Substance	Purity [%]	ρ [kg m^{-3}]		u [m s^{-1}]		η [10^{-3} Pa s]	
		This work	Lit.	This work	Lit.	This work	Lit.
ethanol	≥ 99.9	785.253	785.46 [6] 785.27 [2]	1143.14	1142.6 [19]	1.082	1.082 [6]
benzene	≥ 99.7	873.689	873.60 [4]	1299.08	1299.73 [4]	0.602	0.604 [4]
pyridine	≥ 99.5	978.050	978.10 [7]	1416.64	1418.2 [7]	0.879	0.882 [7]

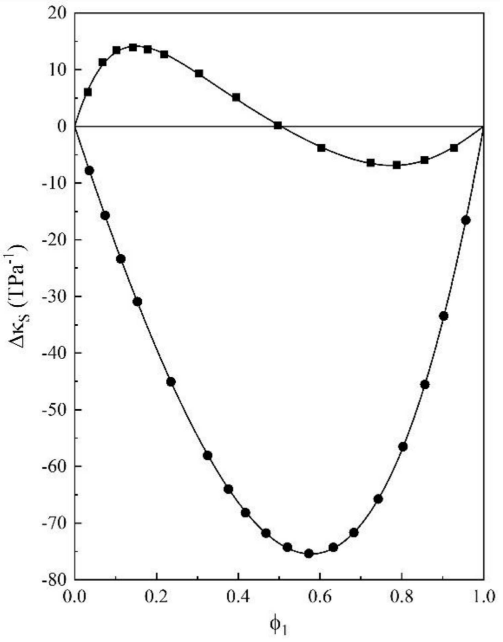

Fig. 1. Deviation in isentropic compressibility, $\Delta\kappa_S$, against the volume fraction of ethanol, φ_1, for the (■) ethanol + benzene and (●) ethanol + pyridine mixtures at 298.15 K and atmospheric pressure. Symbols refer to experimental data points; solid lines are the results calculated from the Redlich–Kister polynomial [20].

With increase in the temperature, the absolute values of $\Delta\kappa_S$ and V^E for both systems increase with the same dependences and systematic variation. Thus, to avoid overcrowding of the curves the results have been presented at $T = 298.15$ K only. The deviations in viscosity $\Delta\eta$ at 298.15 K are negative for both systems over the entire composition range. We can observe that for ethanol + benzene system the $\Delta\eta$–x_1 curve exhibits a parabolic-like dependence with a minimum value located at $x_1 \approx 0.5$.

In Fig. 2, the literature values of Han et al. [2], Šerbanović et al. [21], and Findlay and Copp [22] are also shown. We can observe that our V^E data agree well with those reported in the literature.

The $\Delta\kappa_S$, V^E, and $\Delta\eta$ data have been fitted by the method of least-squares with the Redlich–Kister type polynomial equation

$$Y = X(1-X)\sum_{j=1}^{k} A_j (1-2X)^{j-1}, \qquad (6)$$

where $X = x_1$ for $Y = V^E$ and $\Delta\eta$, $X = \varphi_1$ for $Y = \Delta\kappa_S$. The number k of adjustable fitting parameters, A_j, needed in Eq. (6) for fitting the $\Delta\kappa_S$, V^E, and $\Delta\eta$ data was optimized by using an F-test at 0.005 significance level [23]. The standard deviations (σ) of the fitting were defined as:

$$\sigma(Y) = \left[\sum (Y_{\text{exp}} - Y_{\text{calc}})^2 / (n-k)\right]^{1/2}, \qquad (7)$$

where n is the number of data points. Y_{exp} and Y_{calc} refer to experimental and calculated values of Y, respectively.

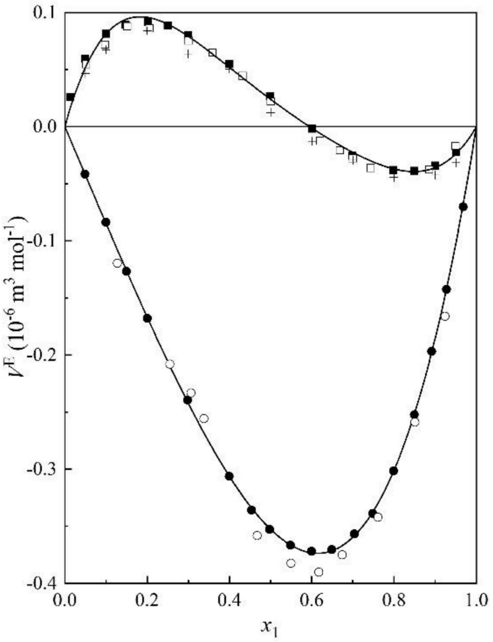

Fig. 2. Excess molar volumes, V^E, against the mole fraction of ethanol, x_1, at 298.15 K and atmospheric pressure, for the ethanol + benzene system: (■) this work, (□) Šerbanović et al. [21], (+) Han et al. [2], and ethanol + pyridine system: (●) this work (○) Findlay and Copp [22]. Symbols refer to experimental data points; solid lines are the results calculated from the Redlich–Kister polynomial [20].

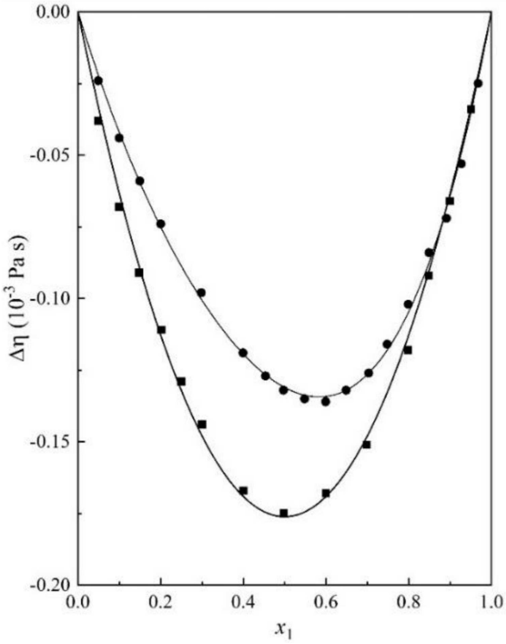

Fig. 3. Viscosity deviations, $\Delta\eta$, against the mole fraction of ethanol, x_1, for the (■) ethanol + benzene and (●) ethanol + pyridine systems at 298.15 K and atmospheric pressure. Symbols refer to experimental data points; solid lines are the results calculated from the Redlich–Kister polynomial [20].

TABLE II

Densities ρ [kg m^{-3}], speeds of sound u [m s^{-1}], excess molar volumes V^E [10^{-6} m^3 mol^{-1}], and deviations in isentropic compressibility $\Delta\kappa_S$ [TPa^{-1}], of ethanol + benzene mixtures at temperature T, against the mole fraction of ethanol, x_1.

x_1	ρ	u	V^E	$\Delta\kappa_S$	x_1	ρ	u	V^E	$\Delta\kappa_S$
T = 293.15 K									
0.0000	879.023	1322.74	0.0000	0.00	0.4982	843.537	1241.87	0.0150	3.74
0.0488	875.576	1309.46	0.0530	6.39	0.6003	834.729	1228.80	−0.0116	−1.15
0.0994	872.245	1297.60	0.0719	11.04	0.6990	825.386	1214.78	−0.0332	−4.77
0.1480	869.057	1288.85	0.0781	12.73	0.7990	814.872	1199.29	−0.0433	−7.17
0.2018	865.451	1280.65	0.0795	12.93	0.8491	809.143	1190.70	−0.0424	−7.29
0.2501	862.145	1273.80	0.0756	12.42	0.9000	802.966	1181.20	−0.0365	−6.25
0.3001	858.645	1266.99	0.0667	11.43	0.9509	796.370	1170.96	−0.0232	−3.93
0.4004	851.275	1254.25	0.0424	7.90	1.0000	789.538	1160.21	0.0000	0.00
T = 298.15 K									
0.0000	873.689	1299.08	0.0000	0.00	0.4982	838.501	1220.78	0.0266	5.13
0.0488	870.221	1286.88	0.0594	6.02	0.6003	829.815	1208.31	−0.0019	0.10
0.0994	866.900	1275.07	0.0813	11.29	0.6990	820.601	1195.01	−0.0255	−3.78
0.1480	863.732	1266.38	0.0892	13.39	0.7990	810.236	1180.31	−0.0380	−6.49
0.2018	860.157	1258.32	0.0917	13.86	0.8491	804.591	1172.16	−0.0387	−6.79
0.2501	856.882	1251.63	0.0885	13.53	0.9000	798.500	1163.14	−0.0341	−5.94
0.3001	853.417	1244.96	0.0802	12.73	0.9509	791.995	1153.39	−0.0221	−3.78
0.4004	846.139	1232.65	0.0551	9.32	1.0000	785.253	1143.14	0.0000	0.00
T = 303.15 K									
0.0000	868.338	1275.58	0.0000	0.00	0.4982	833.421	1199.94	0.0404	6.54
0.0488	864.846	1264.46	0.0662	5.59	0.6003	824.857	1188.03	0.0098	1.41
0.0994	861.531	1252.65	0.0916	11.58	0.6990	815.776	1175.39	−0.0164	−2.67
0.1480	858.379	1244.05	0.1015	14.10	0.7990	805.565	1161.50	−0.0321	−5.76
0.2018	854.831	1236.18	0.1055	14.82	0.8491	799.999	1153.75	−0.0339	−6.19
0.2501	851.585	1229.64	0.1031	14.69	0.9000	793.997	1145.19	−0.0310	−5.52
0.3001	848.156	1223.20	0.0951	13.99	0.9509	787.586	1135.95	−0.0207	−3.59
0.4004	840.960	1211.33	0.0701	10.71	1.0000	780.937	1126.21	0.0000	0.00
T = 308.15 K									
0.0000	863.001	1251.97	0.0000	0.00	0.4982	828.301	1179.32	0.0577	7.80
0.0488	859.451	1242.11	0.0765	4.90	0.6003	819.855	1167.98	0.0247	2.60
0.0994	856.135	1230.66	0.1059	11.26	0.6990	810.907	1155.94	−0.0046	−1.58
0.1480	852.996	1222.13	0.1181	14.27	0.7990	800.849	1142.76	−0.0239	−4.88
0.2018	849.471	1214.29	0.1236	15.48	0.8491	795.367	1135.44	−0.0277	−5.49
0.2501	846.251	1208.02	0.1222	15.43	0.9000	789.455	1127.34	−0.0268	−5.00
0.3001	842.855	1201.72	0.1146	14.97	0.9509	783.141	1118.60	−0.0187	−3.28
0.4004	835.741	1190.22	0.0891	11.94	1.0000	776.590	1109.43	0.0000	0.00
T = 313.15 K									
0.0000	857.66	1228.39	0.0000	0.00	0.4982	823.13	1158.84	0.0782	9.07
0.0488	854.04	1220.05	0.0887	3.78	0.6003	814.81	1147.99	0.0421	3.90
0.0994	850.71	1208.92	0.1225	10.58	0.6990	805.98	1136.60	0.0101	−0.44
0.1480	847.58	1200.49	0.1373	14.09	0.7990	796.09	1124.12	−0.0141	−3.96
0.2018	844.08	1192.74	0.1447	15.76	0.8491	790.69	1117.23	−0.0201	−4.77
0.2501	840.88	1186.45	0.1443	16.21	0.9000	784.87	1109.63	−0.0217	−4.55
0.3001	837.52	1180.46	0.1370	15.76	0.9509	778.66	1101.40	−0.0164	−3.09
0.4004	830.48	1169.34	0.1113	13.02	1.0000	772.20	1092.72	0.0000	0.00

TABLE III

Densities ρ [kg m^{-3}], speeds of sound u [m s^{-1}], excess molar volumes V^E [10^{-6} m^3 mol^{-1}], and deviations in isentropic compressibility $\Delta\kappa_S$ [T Pa^{-1}], of ethanol + pyridine mixtures at temperature T, against the mole fraction of ethanol, x_1.

x_1	ρ	u	V^E	$\Delta\kappa_S$	x_1	ρ	u	V^E	$\Delta\kappa_S$
$T = 293.15$ K									
0.0000	983.081	1437.09	0.0000	0.00	0.5994	887.278	1312.69	-0.3724	-71.82
0.0491	976.600	1429.38	−0.0410	−7.55	0.6489	877.160	1298.27	−0.3709	−72.95
0.1001	969.663	1420.81	−0.0830	−15.14	0.7037	865.401	1280.86	−0.3575	−71.88
0.1498	962.725	1412.30	−0.1259	−22.57	0.7482	855.434	1266.01	−0.3398	−69.44
0.2004	955.413	1403.09	−0.1670	−29.84	0.7990	843.451	1247.58	−0.3026	−63.71
0.2984	940.494	1384.45	−0.2384	−43.50	0.8491	831.047	1227.98	−0.2534	−54.69
0.3996	924.017	1363.21	−0.3054	−56.14	0.8916	819.997	1210.36	−0.1978	−44.09
0.4540	914.631	1350.59	−0.3352	−61.82	0.9275	810.306	1194.49	−0.1432	−32.35
0.4975	906.795	1340.15	−0.3522	−65.90	0.9681	798.907	1175.76	−0.0707	−15.98
0.5480	897.343	1326.89	−0.3665	−69.37	1.0000	789.538	1160.21	0.0000	0.00
$T = 298.15$ K									
0.0000	978.050	1416.64	0.0000	0.00	0.5994	882.564	1293.42	−0.3720	−74.23
0.0491	971.594	1408.97	−0.0415	−7.81	0.6489	872.484	1279.16	−0.3705	−75.37
0.1001	964.683	1400.54	−0.0838	−15.72	0.7037	860.768	1262.00	−0.3568	−74.27
0.1498	957.768	1392.09	−0.1269	−23.40	0.7482	850.839	1247.30	−0.3389	−71.68
0.2004	950.480	1383.00	−0.1680	−30.95	0.7990	838.904	1229.15	−0.3015	−65.77
0.2984	935.610	1364.53	−0.2395	−45.09	0.8491	826.554	1209.89	−0.2523	−56.52
0.3996	919.185	1343.42	−0.3062	−58.09	0.8916	815.556	1192.53	−0.1968	−45.57
0.4540	909.829	1331.00	−0.3359	−64.02	0.9275	805.912	1176.92	−0.1425	−33.47
0.4975	902.020	1320.62	−0.3528	−68.19	0.9681	794.571	1158.48	−0.0703	−16.56
0.5480	892.597	1307.52	−0.3667	−71.77	1.0000	785.253	1143.14	0.0000	0.00
$T = 303.15$ K									
0.0000	973.008	1396.22	0.0000	0.00	0.5994	877.826	1274.25	−0.3716	−76.72
0.0491	966.575	1388.70	−0.0418	−8.15	0.6489	867.780	1260.17	−0.3697	−77.88
0.1001	959.686	1380.33	−0.0843	−16.33	0.7037	856.106	1243.20	−0.3557	−76.69
0.1498	952.795	1371.97	−0.1277	−24.30	0.7482	846.215	1228.75	−0.3377	−74.06
0.2004	945.529	1362.98	−0.1688	−32.12	0.7990	834.330	1210.90	−0.3004	−67.99
0.2984	930.705	1344.64	−0.2402	−46.71	0.8491	822.033	1191.90	−0.2511	−58.38
0.3996	914.330	1323.75	−0.3067	−60.16	0.8916	811.086	1174.85	−0.1958	−47.13
0.4540	905.003	1311.49	−0.3362	−66.31	0.9275	801.487	1159.50	−0.1416	−34.65
0.4975	897.218	1301.18	−0.3529	−70.57	0.9681	790.206	1141.32	−0.0700	−17.13
0.5480	887.826	1288.29	−0.3665	−74.32	1.0000	780.937	1126.21	0.0000	0.00
$T = 308.15$ K									
0.0000	967.974	1375.75	0.0000	0.00	0.5994	873.060	1255.36	−0.3701	−79.54
0.0491	961.543	1368.54	−0.0406	−8.62	0.6489	863.050	1241.31	−0.3682	−80.54
0.1001	954.675	1360.27	−0.0833	−17.11	0.7037	851.415	1224.60	−0.3539	−79.31
0.1498	947.805	1351.97	−0.1268	−25.34	0.7482	841.564	1210.27	−0.3360	−76.46
0.2004	940.561	1343.08	−0.1681	−33.45	0.7990	829.725	1192.77	−0.2986	−70.28
0.2984	925.780	1324.88	−0.2396	−48.50	0.8491	817.481	1174.07	−0.2495	−60.35
0.3996	909.452	1304.21	−0.3059	−62.39	0.8916	806.584	1157.28	−0.1944	−48.70
0.4540	900.153	1292.02	−0.3353	−68.67	0.9275	797.033	1142.15	−0.1406	−35.76
0.4975	892.392	1281.80	−0.3519	−73.03	0.9681	785.810	1124.27	−0.0695	−17.66
0.5480	883.029	1269.11	−0.3653	−76.94	1.0000	776.590	1109.43	0.0000	0.00

TABLE III cont.

x_1	ρ	u	V^E	$\Delta\kappa_S$	x_1	ρ	u	V^E	$\Delta\kappa_S$
$T = 313.15$ K									
0.0000	962.940	1355.32	0.0000	0.00	0.5994	868.265	1236.42	−0.3681	−82.35
0.0491	956.499	1348.44	−0.0384	−9.14	0.6489	858.290	1222.69	−0.3663	−83.53
0.1001	949.651	1340.25	−0.0814	−17.93	0.7037	846.695	1206.14	−0.3519	−82.15
0.1498	942.800	1332.05	−0.1252	−26.47	0.7482	836.879	1191.96	−0.3339	−79.11
0.2004	935.575	1323.24	−0.1665	−34.86	0.7990	825.087	1174.75	−0.2966	−72.75
0.2984	920.834	1305.24	−0.2381	−50.44	0.8491	812.896	1156.33	−0.2478	−62.45
0.3996	904.549	1284.55	−0.3043	−64.55	0.8916	802.047	1139.80	−0.1929	−50.38
0.4540	895.277	1272.67	−0.3336	−71.22	0.9275	792.543	1124.90	−0.1396	−36.98
0.4975	887.539	1262.54	−0.3502	−75.68	0.9681	781.376	1107.33	−0.0691	−18.29
0.5480	878.204	1250.01	−0.3635	−79.71	1.0000	772.204	1092.72	0.0000	0.00

TABLE IV

Dynamic viscosities η [10^{-3} Pa s], and deviations in viscosity $\Delta\eta$ [10^{-3} Pa s], of ethanol + benzene and ethanol + pyridine mixtures at temperature 298.15 K, against the mole fraction of ethanol, x_1.

x_1	η	$\Delta\eta$	x_1	η	$\Delta\eta$
Ethanol + benzene					
0.0000	0.602	0.000	0.4982	0.666	−0.175
0.0488	0.587	−0.038	0.6003	0.722	−0.168
0.0994	0.582	−0.068	0.6990	0.786	−0.151
0.1480	0.582	−0.091	0.7990	0.868	−0.118
0.2018	0.587	−0.111	0.8491	0.917	−0.092
0.2501	0.593	−0.129	0.9000	0.968	−0.066
0.3001	0.602	−0.144	0.9509	1.024	−0.034
0.4004	0.627	−0.167	1.0000	1.082	0.000
Ethanol + pyridine					
0.0000	0.879	0.000	0.5994	0.865	−0.136
0.0491	0.866	−0.024	0.6489	0.879	−0.132
0.1001	0.856	−0.044	0.7037	0.896	−0.126
0.1498	0.850	−0.059	0.7482	0.915	−0.116
0.2004	0.846	−0.074	0.7990	0.940	−0.102
0.2984	0.842	−0.098	0.8491	0.967	−0.084
0.3996	0.841	−0.119	0.8916	0.988	−0.072
0.4540	0.844	−0.127	0.9275	1.015	−0.053
0.4975	0.848	−0.132	0.9681	1.050	−0.025
0.5480	0.855	−0.135	1.0000	1.082	0.000

The fitting parameters, A_j, and the corresponding standard deviations, σ, for the $\Delta\kappa_S$, V^E, and $\Delta\eta$ data of the present investigation are summarized in Table V. The solid lines in Figs. 1–3 refer to the values calculated from Eq. (6) using the corresponding parameters A_j given in Table V. We can observe that there is an excellent agreement between the experimental data and the solid lines calculated with the adjustable parameters. In general, the number of adjustable fitting parameters depends on various factors such as the shape of data across the graph, the number of data points, the quality of the experimental data, and the level of significance. For example, since $\Delta\eta$ data of the ethanol + benzene system showed a parabolic-like dependence with a minimum at ≈ 0.5, only one parameter was needed to fit them significantly. More parameters were needed to fit $\Delta\kappa_S$ and V^E data significantly as they exhibited sine-like behavior.

The observed variations of $\Delta\kappa_S$ and V^E in the present study can be explained qualitatively in terms of several effects, which can be divided into three types: physical, chemical, and structural [3, 5, 21]. The physical interactions comprise mainly of dispersion forces resulting in positive $\Delta\kappa_S$ and V^E values. Chemical contributions include: (i) specific interactions such as formation of hydrogen bonds, charge-transfer complexes, and strong dipole–dipole interactions between the component molecules in the mixture leading to negative $\Delta\kappa_S$ and V^E, and (ii) the stretching and breaking of molecular associates present in the pure liquids giving a positive contribution to $\Delta\kappa_S$ and V^E. The structural contributions include the geometrical interstitial accommodation of molecules into each other's structure due to differences in molar masses, shape, and free volume of the component molecules of the mixtures, resulting in negative trend to $\Delta\kappa_S$ and V^E.

The positive values of $\Delta\kappa_S$ and V^E (see Figs. 1 and 2) in the benzene rich region of the ethanol + benzene system can be attributed mainly to the disruption of the hydrogen-bonded ethanol structures as the ethanol molecules were added to a large amount of benzene. The negative $\Delta\kappa_S$ and V^E values in the ethanol rich region indicate that complex formation occurred through π•••HO bonding between the π-electron cloud of the aromatic ring of benzene and the proton of the hydroxyl group of ethanol. A further negative contribution may have arisen from the interstitial accommodation of benzene molecules into the remaining hydrogen-bonded ethanol structure.

The negative trend over the entire composition range in $\Delta\kappa_S$ and V^E (see Figs. 1 and 2) for the ethanol + pyridine system can be attributed mainly to the formation of complexes by strong cross-associated N• • •HO interactions between the free lone electron pair of

TABLE V

Adjustable fitting parameters, A_j, and standard deviations, σ (Eq. (7)), for mathematical representation with Redlich–Kister polynomials, Eq. (6), of excess molar volumes, V^E [10^{-6} m^3 mol^{-1}], deviations in isentropic compressibility, $\Delta\kappa_S$ [T Pa^{-1}], and deviations in dynamic viscosity, $\Delta\eta$ [10^{-3} Pa s] data, for ethanol + benzene and ethanol + pyridine mixtures at different temperatures, T, under local atmospheric pressure

T [K]	Property	A_0	A_1	A_2	A_3	A_4	A_5	σ
Ethanol + benzene								
293.15	V^E	0.0506	0.5106	0.2131	0.3951			0.0041
	$\Delta\kappa_S$	−4.22	84.81	30.96	18.73	64.77	61.22	0.19
298.15	V^E	0.0960	0.5363	0.2425	0.4316			0.0044
	$\Delta\kappa_S$	0.68	82.39	34.23	63.54	57.98		0.28
	$\Delta\eta$	−0.704						0.003
303.15	V^E	0.1497	0.5644	0.2707	0.4668			0.0047
	$\Delta\kappa_S$	3.87	85.74	67.17	63.55			0.49
308.15	V^E	0.2169	0.5951	0.3222	0.5334			0.0057
	$\Delta\kappa_S$	9.09	90.44	64.60	51.83			0.49
313.15	V^E	0.2961	0.6250	0.3828	0.6192			0.0069
	$\Delta\kappa_S$	14.75	95.32	58.24	36.73			0.65
Ethanol + pyridine								
293.15	V^E	−1.4089	0.7090	−0.1457				0.0012
	$\Delta\kappa_S$	−284.65	90.77	−17.41				0.09
298.15	V^E	−1.4106	0.6978	−0.1415				0.0012
	$\Delta\kappa_S$	−294.28	93.04	−18.59				0.10
	$\Delta\eta$	−0.524	0.154	−0.104				0.002
303.15	V^E	−1.4108	0.6872	−0.1373				0.0013
	$\Delta\kappa_S$	−304.29	93.42	−20.25	5.40			0.10
308.15	V^E	−1.4068	0.6827	−0.1246				0.0013
	$\Delta\kappa_S$	−314.91	97.08	−21.77				0.11
313.15	V^E	−1.4002	0.6825	−0.1087				0.0015
	$\Delta\kappa_S$	−326.16	99.31	−24.01				0.11

electronegative N-atom of pyridine and the proton of the hydroxyl group of ethanol. Additional negative contributions to $\Delta\kappa_S$ and V^E arise from $\pi \bullet \bullet\bullet$HO bond formation between the ethanol molecules and delocalized π-electrons of the aromatic ring of pyridine, and structural effects. Similar results are also obtained by Anwar et al. [3] for binary mixtures of pyridine with 1-alkanols (C_6–C_{10}), and by Kijevčanin et al. [10] for mixtures of pyridine with 1-propanol and 1,2-propanediol.

The effect of temperature on $\Delta\kappa_S$ and V^E for both systems is worthy of notice. In liquid mixtures, there is always a competition between molecular interactions and disordered thermal movement of molecules. Increasing thermal movement of molecules with increasing temperature will result in the decrease of molecular interactions, weakening of molecular associations, and to the decrease of the number of cross-associated complexes through $\pi \bullet\bullet\bullet$HO and N$\bullet\bullet\bullet$ HO bonding. This explains the systematic increase of the absolute values of $\Delta\kappa_S$ and V^E with the rising of temperature in both studied systems.

The observed negative values of $\Delta\eta$ (see Fig. 3) over the entire composition range indicate that in both studied systems the weak dispersion and dipole–dipole forces are predominant, but they may also occur in systems where components are known to interact more strongly, as in our case of ethanol + pyridine system. Similar deviations in $\Delta\eta$ from ideal behaviour have also been suggested by Anwar et al. [3] for binary mixtures of pyridine and alkanols (C_6–C_{10}) at 303.15 K, and by Garcia et al. [24] for mixtures of *N*-methylpyrrolidine and alkanols (C_1–C_{10}) at 298.15 K.

4. Conclusion

This paper reports experimental data for density ρ and speed of sound u, at $T = 293.15$, 298.15, 303.15, 308.15, and 313.15 K, and viscosity η, at $T = 298.15$ K, under local atmospheric pressure of ≈ 95 kPa, for ethanol + benzene and ethanol + pyridine mixtures over the entire composition range. From experimental data, the excess molar volumes V^E, deviations in isentropic compressibility $\Delta\kappa_S$, and viscosity deviations from ideal behavior $\Delta\eta$ have been derived and fitted by the method of least-squares with the Redlich–Kister type polynomials. Excellent agreement was achieved between experimental $\Delta\kappa_S$, V^E, and $\Delta\eta$, and the results calculated by Redlich–Kister polynomials. The $\Delta\kappa_S$ and V^E values are negative over the entire composition range in ethanol + pyridine system, whereas in ethanol + benzene system the $\Delta\kappa_S$

and V^E exhibit a sigmoidal S-shaped composition dependence. This kind of behavior could be interpreted in terms of various balancing contributions arising from physical, chemical, and structural effects. The $\Delta\eta$ values are negative for both systems with a minimum located between 0.5 and 0.6 mol fractions of ethanol.

References

[1] H.W. Chen, C.H. Tu, *J. Chem. Eng. Data* **50**, 1262 (2005).

[2] K.J. Han, J.H. Oh, S.J. Park, *J. Ind. Eng. Chem.* **13**, 360 (2007).

[3] A. Ali, M. Tariq, F. Nabi, Shahjahan, *Chin. J. Chem.* **26**, 2009 (2008).

[4] J.A. Al-Kandary, A.S. Al-Jimaz, A.H.M. Abdul-Latif, *J. Chem. Eng. Data* **51**, 2074 (2006).

[5] G.P. Dubey, M. Sharma, N. Dubey, *J. Chem. Thermodyn.* **40**, 309 (2008).

[6] B. González, N. Calvar, E. Gómez, Á. Domínguez, *J. Chem. Thermodyn.* **39**, 1578 (2007).

[7] M.S. Bakshi, G. Kaur, *J. Chem. Eng. Data* **42**, 298 (1997).

[8] H.G. Franck, J.W. Stadelhofer, in: *Industrial Aromatic Chemistry*, Springer, Heidelberg 1988, p. 132.

[9] J.A. Joule, K. Mills, *Heterocyclic Chemistry*, 5th ed., Wiley-Blackwell, West Sussex 2010.

[10] M.L. Kijevčanin, E.M. Živković, B.D. Djordjević, I.R. Radović, J. Jovanović, S.P. Šerbanović, *J. Chem. Thermodyn.* **56**, 49 (2013).

[11] S. Shimizu et al., *Pyridine and Pyridine Derivatives*, in: *Ullmann's Encyclopedia of Industrial Chemistry*, Vol. 30, Wiley-VCH, Weinheim 2000, p. 557.

[12] J.M. Vuksanovic, D.M. Bajic, G.R. Ivanis, E.M. Zivkovic, I.R. Radovic, S.P. Serbanovic, M.Lj. Kijevcanin, *J. Serbian Chem. Soc.* **79**, 707 (2014).

[13] A. Ali, A.K. Nain, B. Lal, D. Chand, *Int. J. Thermophys.* **25**, 1835 (2004).

[14] F. Aliaj, N. Syla, A.B. Damoni, in: *Proc. 3rd Virtual Conf. QUAESTI*, Zilina (Slovakia) 2015, p. 216.

[15] F. Aliaj, A.B. Damoni, N. Syla, *AKTET J. Inst. Alb-Shkenca* **9**, 36 (2016).

[16] F. Aliaj, A. Bytyqi-Damoni, N. Syla, *AIP Conf. Proc.* **1722**, 290015 (2016).

[17] F. Aliaj, N. Syla, A. Bytyqi-Damoni, in: *Proc. 2nd Int. Conf. on Computational and Experimental Science and Engineering (ICCESEN 2015)*, Antalya (Turkey) 2015.

[18] A. Zeqiraj, F. Aliaj, N. Syla, in: *Proc. 4th Int. Conf. on Computational and Experimental Science and Engineering (ICCESEN 2017)*, Antalya (Turkey), 2017.

[19] J. Canosa, A. Rodríguez, J. Tojo, *J. Chem. Eng. Data* **43**, 961 (1998).

[20] O. Redlich, A.T. Kister, *Ind. Eng. Chem.* **40**, 345 (1948).

[21] S.P. Šerbanović, M.L. Kijevčanin, I.R. Radović, B.D. Djordjević, *Fluid Phase Equilib.* **239**, 69 (2006).

[22] T.J.V. Findlay, J.L. Copp, *Trans. Faraday Soc.* **65**, 1463 (1969).

[23] P.R. Bevington, D.K. Robinson, *Data Reduction and Error Analysis for the Physical Sciences*, 3rd ed., McGraw-Hill, New York 2003.

[24] B. García, R. Alcalde, S. Aparicio, J.M. Leal, *Phys. Chem. Chem. Phys.* **4**, 1170 (2002).